Article

Three-Phase Catalytic Hydrogenation of a Functionalized Alkyne: Mass Transfer and Kinetic Studies with in Situ Hydrogen Monitoring

Andrea Bruehwiler, Natalia Semagina, Martin Grasemann, Albert Renken, Lioubov Kiwi-Minsker, Axel Saaler, Hajo Lehmann, Werner Bonrath, and Felix Roessler

More About This Article

Additional resources and features associated with this article are available within the HTML version:

- Supporting Information
- Access to high resolution figures
- Links to articles and content related to this article
- Copyright permission to reproduce figures and/or text from this article

View the Full Text HTML

Three-Phase Catalytic Hydrogenation of a Functionalized Alkyne: Mass Transfer and Kinetic Studies with in Situ Hydrogen Monitoring

Andrea Bruehwiler, Natalia Semagina, Martin Grasemann, Albert Renken, and Lioubov Kiwi-Minsker*

Group of Catalytic Reaction Engineering, Ecole Polytechnique Fédérale de Lausanne, GGRC-EPFL, Station 6, CH-1015 Lausanne, Switzerland

Axel Saaler, Hajo Lehmann, Werner Bonrath, and Felix Roessler

DSM Nutritional Products, CH-4303 Kaiseraugst, Switzerland

Systematic studies of mass transfer interactions with intrinsic reaction kinetics were performed for the three-phase selective hydrogenation of 2-methyl-3-butyn-2-ol (MBY) to 2-methyl-3-buten-2-ol (MBE) over a modified Pd/CaCO$_3$ catalyst under solvent free conditions. Hydrogen concentration in the liquid phase ($C_{H2,b}$) was monitored in situ during the catalytic reaction by means of the "Fugatron" analyzer. Reactions were carried out in an autoclave at different stirring rates at two concentrations of hydrogen (5 and 13 mol·m^{-3}). For stirring speeds higher than 1500 rpm no influence of gas–liquid mass transfer was observed. Hydrogen liquid–solid (L-S) mass transfer was found to be negligible, whereas the MBY mass L-S transfer becomes important at high MBY conversions at high hydrogen concentration. Low stirrer speed caused the reaction rate and MBE selectivity to decrease. No internal mass transfer limitations were observed, and conditions for the kinetic regime were found. The kinetics modeled followed the Langmuir–Hinshelwood mechanism and was consistent with the experimental data.

1. Introduction

Three-phase catalytic selective hydrogenations are key processes in fine chemicals production.[1−7] They are often carried out in semibatch autoclaves under elevated pressure with powdered catalysts. The efficiency of these processes is strongly dependent not only on the catalysts' intrinsic activity and selectivity but also on the interaction of mass/heat transfer with the chemical kinetics. Some studies have been devoted to the analysis of mass transfer and its influence on the overall kinetics in three-phase hydrogenations.[8−12] External gas–liquid (G-L) and liquid–solid (L-S), as well as internal, mass transfers often control the reaction kinetics over active catalysts leading to lower reaction rates and selectivities.[12] Both mass transfer and kinetics are sometimes modeled simultaneously, which complicates the correct estimation of the kinetic parameters. Therefore, the reaction conditions ensuring the intrinsic kinetic regime are important for maximum process efficiency and for the understanding of the reaction mechanism.

In the case of hydrogenations, the problem of a reliable G-L mass transfer characterization is due to the difficulty of monitoring the hydrogen concentration in the liquid phase under reaction conditions.[13] Often, the extent of the G-L mass transfer limitation is estimated on the basis of a volumetric mass transfer coefficient ($k_L \cdot a$) derived from measurements made in liquids containing only noncatalytic suspended particles or no particles at all. This brings numerous uncertainties for the analysis under real reaction conditions.[14,15] Recently, in situ measurements of dissolved hydrogen during the liquid-phase hydrogenations were performed using a Fugatron (DMP Ltd., Switzerland) analyzer. The instrument contains a probe with a tip consisting of a porous metal substrate coated with a dense layer of fluoropolymer. It is immersed into a liquid phase, from where the hydrogen molecules permeate into a carrier gas stream used to purge the probe internally. The concentration in the carrier gas stream is measured by a gas analyzer. The instrument performance and the data reliability were discussed in detail by Meyberg and Roessler.[14] Feasibility of its application for measuring ($k_L \cdot a$) was shown for a Co-catalyzed reduction of aliphatic dinitrile to the corresponding diamine[16] and a Pd-catalyzed hydrogenation of a liquid alkyne.[14] In situ measurements of a dissolved hydrogen concentration by Fugatron allow evaluation the G-L mass transfer limitations in a straightforward manner. The influence of the dissolved hydrogen concentrations on the reaction rate and selectivity is of high importance during chemical process development, as well as for the reactor scale-up and optimization.[14] No systematic studies of mass transfer and kinetics during three-phase hydrogenations with in situ hydrogen concentration monitoring have been performed so far.

The present work is aimed at studying external (G-L and L-S) and internal mass transfer, as well as the intrinsic kinetics of three-phase Pd/CaCO$_3$-catalyzed selective hydrogenation of 2-methyl-3-butyn-2-ol (MBY) to 2-methyl-3-buten-2-ol (MBE) (see the reaction scheme in Figure 1). MBE is an important
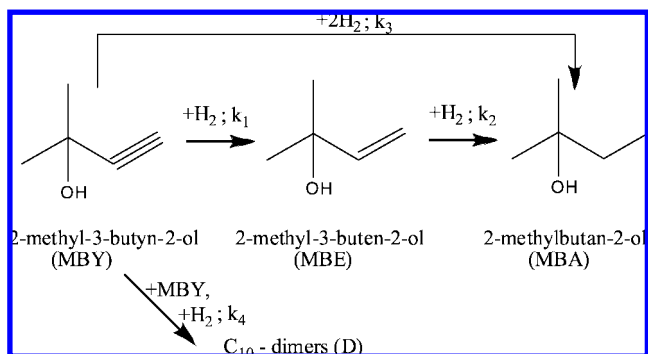

Figure 1. Reaction scheme of 2-methyl-3-butyn-2-ol hydrogenation with the rate constants k_i.

* To whom correspondence should be addressed. E-mail: lioubov.kiwi-minsker@epfl.ch.

Table 1. Some Physical Properties of the Used Materials

	density, ρ (kg·m^{-3})		viscosity, $\mu \times 10^3$ (Pa·s)		vapor pressure, $p \times 10^{-5}$ (Pa)		molecular diffusivity,^{b} $D \times 10^9$ (m^2·s^{-1})	
	293 K	333 K	293 K	333 K	333 K	293 K	303 K	333 K
MBY	865	821	3.38	1.04	0.16		0.59	1.47
MBE		784	1.68^a	0.74				
H$_2$						7.9		29.2

^{a} At 303 K. ^{b} MBY molecular diffusivity in the reaction mixture $D_{MBY,MBE}$ at 303 K was assumed to be identical to the methanol/1-butanol system.[20] Molecular diffusivity of H$_2$ in the reaction mixture at 293 K was assumed to be identical to H$_2$ in 1-methyl-1-propanol.[21] The molecular diffusivities at 333 K were estimated using eq 5.

intermediate in the synthesis of vitamins A and E and perfumes.[17] Solvent free conditions were applied as done on an industrial scale, while a majority of the existent studies of similar reactions are performed in a solvent[12,18,19] giving rise to solvent effects.[11] For the first time the thorough study of a three-phase reaction was performed using in situ monitoring of the dissolved hydrogen concentration via Fugatron. It allowed quantitatively determining G-L mass transfer coefficients without and with catalyst particles, as well as estimating the mass transfer enhancement in the catalyst presence. Kinetic modeling could be performed ensuring the intrinsic kinetic regime for the conditions applied.

2. Experimental Section

2.1. Materials. 2-Methyl-3-butyn-2-ol (MBY) and hydrogen are of 99.73% and 99.995% purity, respectively. Physical properties of MBY, MBE, and H$_2$ are provided in Table 1 (the properties were measured at DSM Nutritional Products at Kaiseraugst/Switzerland, unless stated otherwise[20,21]). H$_2$ partial pressure is $p_{H2} \approx (p_{total} - p_{MBY})$ Pa. The H$_2$ Henry coefficient in the substrate was determined by gas absorption measurements as $H_{H2,MBY}$ (333 K) = 4.40×10^4 Pa·m^3·mol^{-1}. The catalyst used was a modified 5 wt % Pd/CaCO$_3$ powder. The catalyst density was assumed to be identical to the particle density of calcite[22] as $\rho_p = 2710$ kg·m^{-3}. The laser diffraction measurements with a Sympatec (Sympatec GmbH, Clausthal, Germany) HELOS (H004) cell were performed to determine the particle size. Two measurements of 10 s each were carried out to ensure reproducibility. The catalyst was suspended in MBY and stirred at 600 rpm before the measurement. The catalyst's porosity was determined using a Sorptomatic 1990 (Carlo Erba Instruments, Italy) instrument via N$_2$ adsorption at 77 K. The calculation was performed following the Dollimore/Heal method.[23]

2.2. On-Line Analysis of the Hydrogen Concentration. The online measurement of the hydrogen concentration in the liquid phase was carried out with a hydrogen analyzer Fugatron HYD-100 (DMP, Switzerland) as described by Meyberg and Roessler.[14] The permeation probe operated with a carrier gas flow of 15 cm^3(STP)·min^{-1}. The active area of the probe was 8 cm^2, and the film thickness was 0.25 mm.

The measured hydrogen concentration in the carrier gas is dependent on the concentration of dissolved hydrogen. On the basis of the Henry coefficient, a quantitative relation between the gas and the liquid phase concentration can be established as shown in Figure 2. The error in estimating the hydrogen concentration in bulk liquid was about 10%. The gas analyzer operates with an accuracy of $\pm 2\%$.[14] To avoid the experimental errors resulting from time response and mass transfer limitations at the probe surface, measurements were taken within an ~8 min period after the sampling by applying a stirring rate above 800 rpm.[14]

2.3. Hydrogenation Reaction. Solvent-free MBY hydrogenations were carried out in a semibatch stainless steel autoclave (250 mL or a 500 mL) equipped with a heating jacket, hydrogen
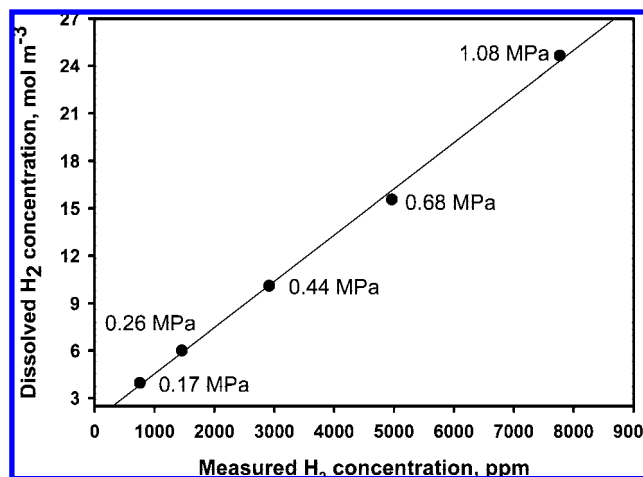
Figure 2. Correlation of the H$_2$ concentration measured by Fugatron with its dissolved concentration in MBY at 333 K and varying pressure (MPa).

supply system, and 8-blade disk turbine impeller of 2.8 cm diameter (d_{st}). Pressure in the reactor was maintained constant during the reaction by a hydrogen feed from the gas reservoir. The hydrogen consumption rate and its conversion were determined based on the known hydrogen supply rate. Pressure values (P) are given as absolute throughout the work. In some experiments, a removable baffle cage was introduced consisting of six baffles over the whole reactor height. To avoid clumping of the catalyst particles, the reaction mixture was stirred for 1 h at 298 K and 2000 rpm in an inert atmosphere before starting the reaction. The measurement of hydrogen concentration in the liquid phase was described in section 2.2.

Samples were periodically withdrawn from the reactor and analyzed by gas chromatography (GC) using a Perkin-Elmer Auto System XL equipped with a 30-m Stabilwax (Crossbond Carbowax-PEG, Restek) 0.32-mm capillary column with a 0.25-μm coating. The carrier gas (He) pressure was 0.1 MPa. Injector and flame ionization detector temperatures were 473 and 523 K, respectively. The oven temperature was maintained at 323 K for 4 min and stepwise increased to 473 at 30 K/min. The GC analysis conditions also allowed detection of the dimer reaction byproducts. Similar GC response factors were assumed for all the compounds based on the fact that the analysis carried out with the use of internal standards (1-butanol) added to samples diluted with water resulted in the same concentrations. The yield of the reaction mixture components Y_i (where i represents MBY, MBE, MBA or D) was defined as $Y_i = A_i/(A_{MBY} + A_{MBE} + A_{MBA} + A_D) \times 100\%$, where A_i is a GC peak area for each component. Molar concentrations C_i were defined using the density of MBY. The MBY conversion was determined as $X = 100\% - Y_{MBY}$. Selectivities to MBE, MBA, and D were calculated as $S_i = Y_i X^{-1} \times 100\%$.

To check the reproducibility, a series of six identical reactions were carried out. The error in initial activity (the rate of MBY

Table 2. MBY Reaction Rates and Hydrogen Concentrations at Different Stirring Speeds (rpm)[a]

	Set 1: $C_{H2,b}$ = 13 mol·m^{-3}				Set 2: $C_{H2,b}$ = 5 mol·m^{-3}			
	1000 rpm	1500 rpm	2000 rpm	2000 rpm baffled	1000 rpm	1500 rpm	2000 rpm	2000 rpm baffled
R_{H2}, mol·kg$_{cat}^{-1}$·s^{-1}	3.5	3.2	3.9	3.8	1.1	1.2	1.2	1.1
p_{H2}, MPa	0.80	0.68	0.68	0.69	0.34	0.27	0.26	0.25
$C_{H2}{}^{*}$, mol·m^{-3}	18.3	15.5	15.5	15.8	7.8	6.2	6.0	5.8

[a] Experimental conditions: 270 g of MBY (reactor volume: 500 mL), 333 K; 45 mg of catalyst, 0.70−0.82 MPa (Set 1); 90 mg of catalyst, 0.27−0.36 MPa (Set 2).

transformation up to 25% conversion) is 3%, MBE selectivity 0.1%, MBA selectivity 4%, and dimer selectivity 2%. The initial activity of the reactor walls was measured in the hydrogenation reaction without adding the catalyst. It was found to be <5% of the activities in the presence of 45 mg catalyst in 270 g of MBY.

2.4. Determination of the Volumetric Gas−Liquid (G-L) Mass Transfer Coefficient (k_L·a). 2.4.1. Experiments in the Absence of the Catalyst, Transient Method. As the response time of the Fugatron is ∼ 3 min,[14] it could not be used for transient experiments which need a time resolution of several seconds. The determination of the volumetric G-L mass transfer coefficient in the absence of catalyst particles (k_L·a)$_0$ was carried out by gas absorption experiments at different stirring speeds as described by Deimling et al.[24] Experiments were performed with 270 g of MBY in a 500 mL reactor at 333 K, with a pressure step from 0.6 to 0.55 MPa. Three experiments were conducted at every stirrer speed. The principle of the gas absorption experiments is provided in the Supporting Information.

2.4.2. Experiments under the Steady State Reaction Conditions. Assuming a steady state hydrogen concentration the volumetric G-L mass transfer coefficient under the reaction conditions (k_L·a)$_r$ can be calculated using eq 1:

$$(k_L·a)_r = \frac{-R_{H2}·m_{Cat}}{(C_{H2}^{*} - C_{H2,b})·V_L}; \quad \text{with} \quad C_{H2}^{*} = \frac{p_{H2}}{H_{H2,MBY}}$$
(1)

where R_{H2} is the transformation rate of hydrogen, mol·kg$_{cat}^{-1}$·s^{-1}; m_{cat} is the catalyst mass, kg; V_L is the liquid phase volume, m^3; $H_{H2,MBY}$ is the Henry constant, Pa·mol^{-1}·m^3, and $C_{H2,b}$ and C_{H2}^{*} are the dissolved and equilibrium hydrogen concentrations, mol·m^{-3}.

Two sets of experiments were performed, one at a dissolved hydrogen concentration of approximately 13 mol·m^{-3} (Set 1) and the other one at approximately 5 mol·m^{-3} (Set 2). These two concentrations were monitored by the Fugatron and adjusted by varying the hydrogen partial pressure. A constant dissolved hydrogen concentration allowed eliminating an intrinsic reaction rate variation due to its proportionality to the hydrogen concentration. Set 1 was performed with 270 g of MBY, 45 mg of the catalyst, 333 K, and a hydrogen pressure of 0.70−0.82 MPa, using a 500 mL reactor. For the Set 2, 90 mg of the catalyst was used, and the hydrogen pressure was varied between 0.27 and 0.36 MPa.

3. Results and Discussion

3.1. Gas−Liquid Mass Transfer. The reaction rates and hydrogen bulk concentrations at different stirring intensities and hydrogen pressures are presented in Table 2. The hydrogen partial pressure decreases with increasing stirrer speed from 1000 to 1500 rpm to ensure equal dissolved hydrogen concentration in the bulk liquid. Above 1500 rpm the same hydrogen partial pressure could be applied (0.68 MPa in Set 1 and 0.26 MPa in
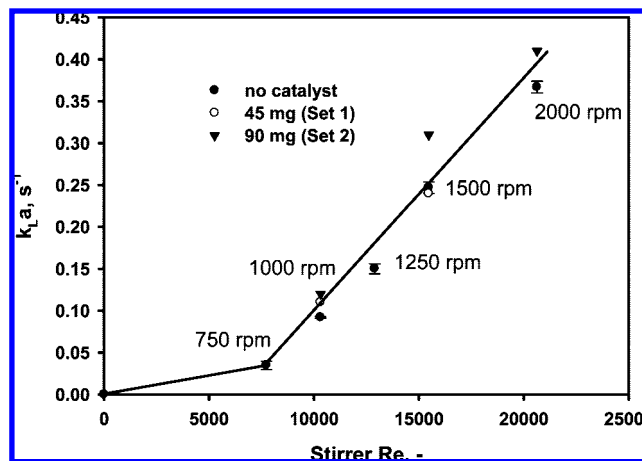

Figure 3. Volumetric G-L mass transfer coefficients as a function of a stirrer Reynolds number in absence and presence of catalyst. Error bars are given for (k_L·a)$_0$ values. Experimental conditions: see section 2.4 and Table 2.

Set 2) resulting in the same $C_{H2,b}$ (Table 2). In consequence, no influence of G-L mass transfer is observed at stirrer speeds above 1500 rpm.

The stirrer Reynolds numbers were determined according to eq 2:[25]

$$Re_{st} = \frac{n·d_{st}^{2}\rho_{MBY}}{\mu_{MBY}}$$
(2)

where n is the rotating speed, s^{-1}.

Volumetric G-L mass transfer coefficients at different stirrer Reynolds numbers are presented in Figure 3 for a system without catalyst (determined by the transient method) and with 45 and 90 mg of catalyst under steady state conditions at the same liquid volume in the reactor. The found (k_L·a) values are reasonable being in the same order of magnitude as reported in the literature for similar systems: 0.03 ± 1.1 s^{-1} for a dinitrile hydrogenation in a 160 mL reactor[16] or 0.1 ± 0.3 s^{-1} for an alkyne hydrogenation in a 500 mL reactor.[14] An important increase of k_L·a is observed for all cases at a stirrer speed of approximately 750 rpm corresponding to the beginning of bubble formation. Error bars are shown in Figure 3 for the (k_L·a)$_0$ values, which are in the range of 1% to 4%. The error in (k_L·a)$_r$ values was between 10% and 30%. This was due to the fact that the term (C_{H2}^{*}− $C_{H2,b}$) in eq 1 is of a low absolute value with the 5% error in C_{H2}* and 10% error in $C_{H2,b}$. Observed volumetric mass transfer coefficients for reacting and nonreacting systems are roughly identical ((k_L·a)$_r$ ≈ (k_L·a)$_0$). No mass transfer enhancement due to the presence of the catalyst particles was observed being in line with published results for particles bigger than 4 μm and at low volumetric solid concentrations.[26]

In summary, G-L mass transfer coefficients (k_L·a) are in the order of 0.35 s^{-1} at a stirrer speed of 2000 rpm. G-L mass transfer is not influencing the global hydrogenation rate at stirrer speeds higher than 1500 rpm for the given reactor setup under the reaction conditions used.

3.2. Liquid−Solid External Mass Transfer. 3.2.1. Carberry Numbers. To estimate the influence of liquid−solid (L-S) mass transfer on the catalytic reaction, the Carberry numbers were calculated, which are a ratio of the observed reaction rate to the maximum mass transfer rate.[27] For the studied reaction, hydrogen is present at low concentration in the liquid phase compared to the organic substances. Therefore, it can be considered as a limiting reactant. The influence of hydrogen L-S mass transfer is estimated for initial reaction conditions. At high conversion, the L-S mass transfer of MBY may also influence the observed rate. MBY mass transfer influence was estimated at maximum MBE yield (ca. 95% MBY conversion).

The L-S mass transfer coefficients k_S, m·s^{-1}, were estimated both for H_2 in MBY and MBY in MBE according to eq 3:

$$k_S = \frac{Sh \cdot D_{2,1}}{d_p} \quad (3)$$

$D_{2,1}$ is the molecular diffusivity of compound 2 in compound 1, m^2 s^{-1}; d_p is the catalyst particle diameter, m; and Sh is the Sherwood number. According to the laser diffraction measurements, the median diameter d_{50} of the catalyst particles is 5.7 μm, while d_5 is 1.3 μm and d_{90} is 14.3 μm. Less then 10% of the catalyst mass is agglomerates of 100 μm. The size of 5.7 μm was taken for the calculations. The molecular diffusivities at 333 K were estimated by applying the Stokes−Einstein equation (eq 4):

$$\frac{D_{2,1,T2} \cdot \mu_{T2}}{T_2} = \frac{D_{2,1,T1} \cdot \mu_{T1}}{T_1} \quad (4)$$

Knowing the viscosities of MBY and MBE at different temperatures, $D_{MBY,MBE}$ at 303 K and $D_{H2,MBY}$ at 293 K (Table 1), the molecular diffusivities of MBY in MBE and H_2 in MBY were determined at 333 K and are presented in Table 1. Higher diffusivity of hydrogen than of organic substrate in ethanol was shown also for three-phase citral hydrogenation.[28]

The Sherwood number was estimated using the Frössling correlation (eq 5) for a slurry containing gas bubbles.[29] The standard deviation on the Sherwood number Sh is predicted to be 31%.

$$Sh = 2 + 0.4 \cdot \left(\frac{Ne \cdot d_I^5 \cdot n_I^3 \cdot d_p^4 \cdot \rho_1^3}{V_L \cdot \mu_1^3} \right)^{1/4} \cdot Sc^{1/3} \quad (5)$$

where Ne is a Newton number taken as 5 from Bates' correlations[30] for a turbine blade stirrer and for a Reynolds number between 10 000 and 20 000; d_I is the stirrer diameter, m; n_I is the stirrer speed, s^{-1}; and ρ is the liquid phase density, kg·m^{-3}. The Schmidt number Sc was estimated using eq 6:

$$Sc = \frac{\mu_1}{\rho_1 \cdot D_{2,1}} \quad (6)$$

The estimated Schmidt number for the diffusion of hydrogen in MBY is $Sc_{H2,MBY} = 43$, while the Schmidt number for the diffusion of MBY in MBE is $Sc_{MBY,MBE} = 642$, indicating that the MBY diffusion is much slower than the diffusion of hydrogen.

The results of the calculations of the mass transfer coefficients are given in Table 3. The mass transfer of a stagnant system was also estimated. Compared to the stagnant liquid, the increase of the mass transfer coefficient due to the agitation is in the order of 20% for hydrogen and 60% for MBY. The mass transfer coefficient of hydrogen is more than 1 order of magnitude higher compared to the mass transfer coefficient of MBY due to the difference in diffusivity of the two components.

Table 3. Sherwood Numbers and Mass Transfer Coefficients for H_2 in MBY and MBY in MBE at 333 K

	stagnant	1000 rpm	1500 rpm	2000 rpm
$Sh_{H2,MBY}$	2	2.2	2.3	2.4
$Sh_{MBY,MBE}$	2	2.7	2.9	3.2
$k_{S,H2} \times 10^3$, m·s^{-1}	10.2	11.4	11.8	12.2
$k_{S,MBY} \times 10^3$, m·s^{-1}	0.52	0.69	0.76	0.82

The Carberry numbers (eqs 7) were estimated for the two sets of experiments at $C_{H2,b} = 13$ mol·m^{-3} and at 5 mol·m^{-3}:

$$Ca_{H2} = \frac{-R_{H2}}{k_{S,H2} \cdot a_S \cdot C_{H2,b}}, \quad Ca_{MBY} = \frac{-R_{MBY}}{k_{S,MBY} \cdot a_S \cdot C_{MBY}} \quad (7)$$

where R_{MBY} is the transformation rate of MBY, mol·kg$_{cat}^{-1}$·s^{-1}, and a_S is the external specific surface area of the catalyst, m^2·kg$_{cat}^{-1}$. The external specific surface area was calculated as 440 m^2 kg$_{cat}^{-1}$ from a spherical particle diameter of 5.7 μm and porosity of 12% (from N_2 adsorption). For the Set 1 of experiments, the following data were used for Ca calculation: $C_{H2,b} = 13.4$ mol·m^{-3}, MBY concentration at the reaction peak (95% conversion) $C_{MBY,peak} = 46$ mol·m^{-3}, initial rate of hydrogen consumption $-R_{H2,init} = 3.6$ mol·kg$_{cat}^{-1}$·s^{-1}, and rate of MBY consumption at its 95% conversion $-R_{MBY,peak} = 5.0$ mol·kg$_{cat}^{-1}$·s^{-1}. For the Set 2: $C_{H2,b} = 5.2$ mol·m^{-3}, $C_{MBY,peak} = 46$ mol·m^{-3}, $-R_{H2,init} = 1.1$ mol·kg$_{cat}^{-1}$·s^{-1}, and $-R_{MBY,peak} = 1.5$ mol·kg$_{cat}^{-1}$·s^{-1}.

The Carberry numbers at different stirrer speeds are presented in Table 4. L-S mass transfer can be neglected at Carberry numbers smaller than 0.05.[27] It follows from Table 4 that hydrogen transfer is not expected to influence the global reaction rate. But, the mass transfer resistance for the alkyne becomes important at its high conversions. However, the Carberry numbers were estimated using the mass transfer coefficients with a standard deviation of 31% and assuming spherical shape of the catalyst particles, while calcium carbonate forms cubes or needles arranged in the hedgehog-like agglomerates of unknown exact structure.[31] Therefore, under- or overestimation of the Carberry numbers cannot be excluded. To verify the predictions, the L-S mass transfer was studied experimentally.

3.2.2. Experimental Study of External L-S Limitations. The measured initial reaction rate is independent of the stirrer speed within the experimental error of ±10% as seen from Table 2. Therefore, the influence of the G-L mass transfer on the overall reaction rate can be neglected.[11] However, selectivity and reaction rates change with stirring rates at higher MBY conversion. Figure 4 shows that at a dissolved hydrogen concentration of $C_{H2,b} = 13$ mol·m^{-3}, the selectivity to MBE increases with the stirring speed, while it is almost not affected at $C_{H2,b} = 5$ mol·m^{-3} by stirring above 1500 rpm. In addition, the observed rate of MBY hydrogenation at $C_{H2,b} = 13$ mol·m^{-3} increases with increasing stirrer speed as seen in Figure 5.

These observations can be explained by the effect of mass transfer of the organic reactants on the reaction rates. Whereas the hydrogen concentration on the catalyst surface is in equilibrium with the bulk concentration, concentration gradients of MBY and MBE can be expected at high conversions (low MBY concentration). This observation is confirmed by the estimated relatively high Carberry numbers for runs carried out at $C_{H2,b} = 13$ mol·m^{-3} (Table 4). Insufficiently fast diffusion of MBY to the catalyst surface from the bulk and of the desorbed MBE to the bulk leads to lower C_{MBY}/C_{MBE} in the L-S diffusion layer compared to the kinetic regime and, thus, to a lower catalyst surface coverage with MBY and higher with MBE.[12]

Table 4. Carberry Numbers at Different Stirring Speeds and Dissolved Hydrogen Concentrations[a]

	Set 1: $C_{H2,b} = 13$ mol·m^{-3}			Set 2: $C_{H2,b} = 5$ mol·m^{-3}		
	1000 rpm	1500 rpm	2000 rpm	1000 rpm	1500 rpm	2000 rpm
Ca_{H2}	0.05	0.05	0.05	0.04	0.04	0.04
Ca_{MBY}	0.36	0.33	0.30	0.11	0.10	0.09

[a] Experimental conditions: see Table 2.
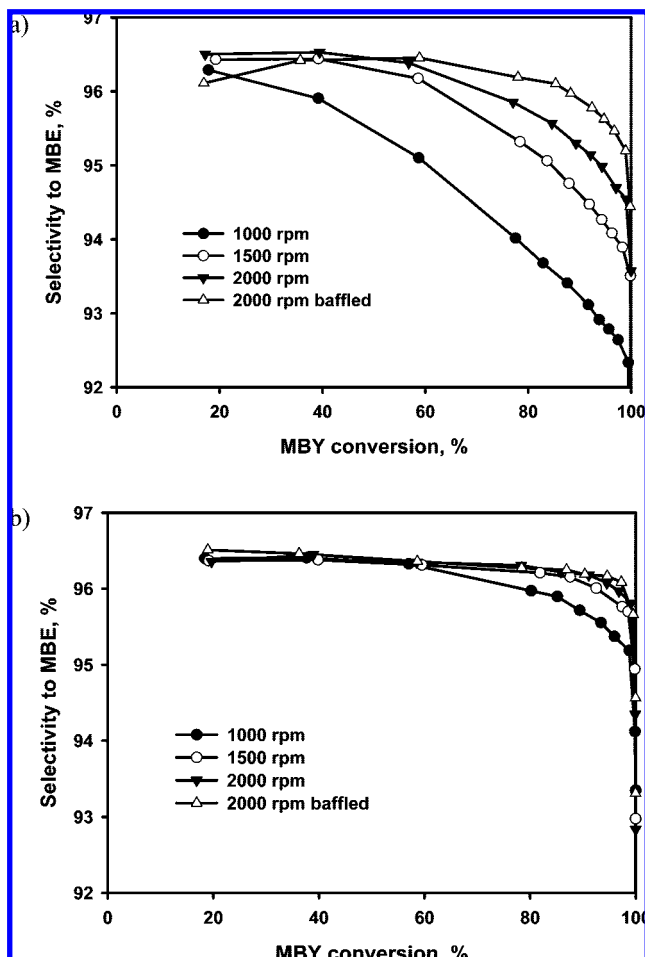
Figure 4. Selectivity to MBE vs MBY conversion during MBY hydrogenation with changing stirrer speeds at the dissolved hydrogen concentrations $C_{H2,b} = 13$ mol·m^{-3} (a) and 5 mol·m^{-3} (b). Experimental conditions: see Table 2.

Therefore, in the case of mass transfer limitations, the overhydrogenation of MBE to MBA starts at a lower MBY conversion. The influence of L-S mass transfer of the organic reactants may explain the reported increase of alkene selectivity with decreasing hydrogen pressures.[32]

3.3. Internal Mass Transfer. The calcium carbonate catalyst support is nonporous. However, the internal mass transfer limitation could be possible inside the large size agglomerates of 100 μm size detected by laser diffraction. To verify the absence of intraparticle mass transfer limitation within the large size agglomerates, the agglomerates were broken up under ultrasonic treatment of the catalyst suspended in MBY. The absence of large aggregates (>50 μm) was confirmed by laser diffraction measurements. Kinetic experiments with and without ultrasonic pretreatment were then compared. The external mass transfer was excluded because the same reaction rates and selectivity for these reactions with and without baffles were obtained.

Figure 6 shows the results of the study for an internal mass transfer process. No difference in catalytic behavior is found
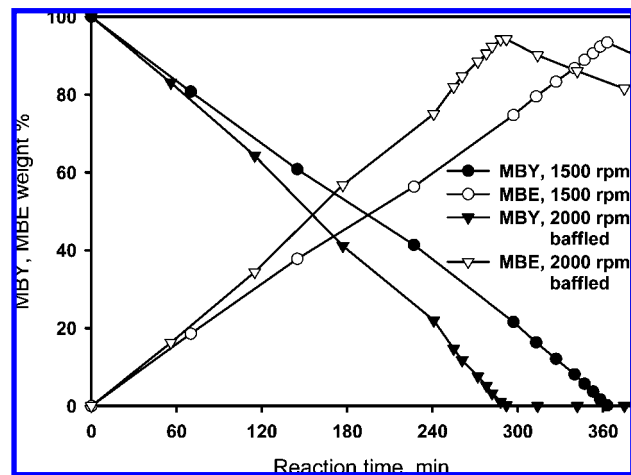

Figure 5. Concentrations of MBY and MBE vs the reaction time during MBY hydrogenation with changing stirrer speeds at the dissolved hydrogen concentration of 13 mol·m^{-3}. Experimental conditions: see Table 2.

between the reaction with and that without ultrasonic pretreatment. Therefore, one can exclude an intraparticle mass transfer limitation.

3.4. Heat Transfer. Analysis of heat transfer is of high importance for highly exothermic hydrogenations. Heat transfer was analyzed considering the worst case of a stagnant liquid around a spherical particle.

The heat transfer coefficient h_S was found from the Fourier's law for heat transfer by conduction as 51 930 W·m^{-2}·K^{-1} assuming a spherical particle of 5.7 μm diameter and the MBY thermal conductivity of 0.148 W·m^{-1}·K^{-1}. The temperature at the catalyst surface T_S was calculated from the heat balance of the system. If the bulk temperature T_b is kept constant, all heat produced by the reaction is transferred from the catalyst surface to the liquid bulk and then evacuated by the walls:

$$-\Delta_r H \cdot r = h_S \cdot a_S (T_S - T_b) \tag{8}$$

where $\Delta_r H$, J·mol^{-1}, is the reaction enthalpy and r, mol·kg$_{cat}^{-1}$·s^{-1}, is the reaction rate.

For $T_b = 333$ K, $\Delta_r H = -170$ kJ mol^{-1} (from a structure-based calculations), $r = 3.6$ mol·kg$_{cat}^{-1}$·s^{-1}, and $a_S = 440$ m^2·kg$_{cat}^{-1}$, T_S was found to be 333.03 K. The calculations show the negligible temperature rise of 0.03 K between bulk liquid and catalyst surface; therefore, the system operates under isothermal conditions.

3.5. Modeling of the Intrinsic Kinetics. At low hydrogen bulk concentration (5 mol·m^{-3}) and high stirrer speed (2000 rpm), mass and heat transfer influences can be neglected. Therefore, the intrinsic kinetics can be modeled under these conditions. A typical Langmuir–Hinshelwood mechanism was used[13,33−35] assuming a competitive adsorption of the reactants on one type of active site and a bimolecular reaction for the species adsorbed. MBA appears in the very beginning of the reaction confirming the presence of a parallel path of MBY hydrogenation to MBA known for acetylene and functionalized
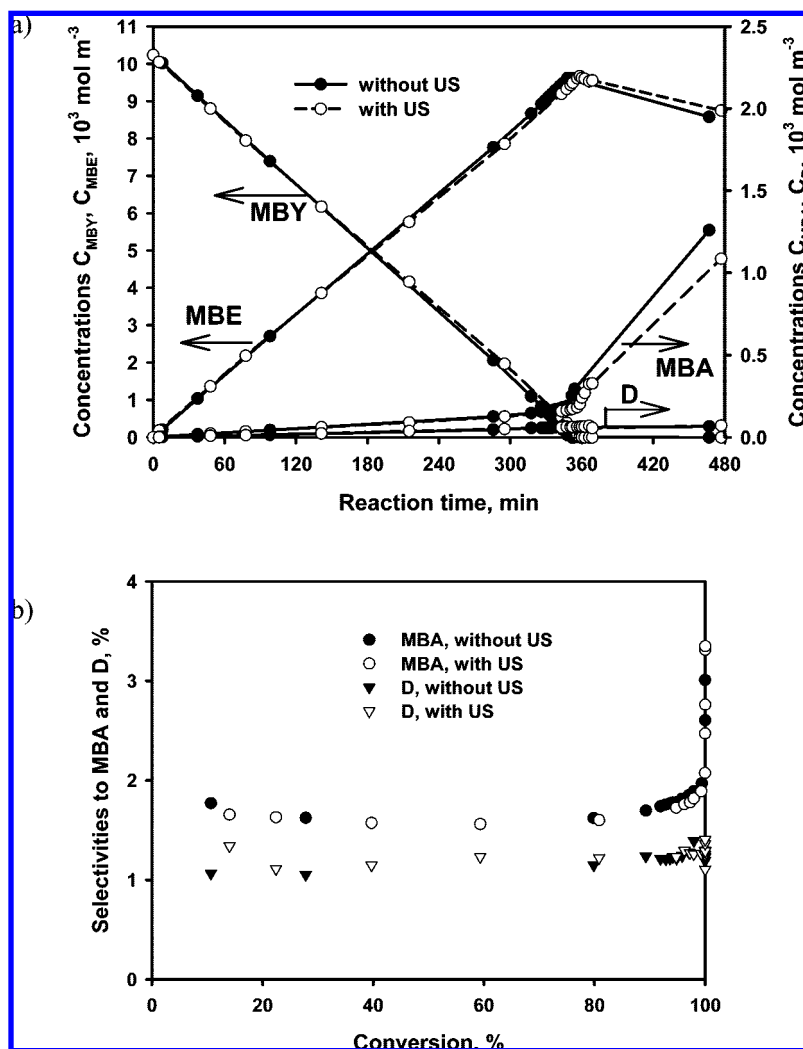
Figure 6. Kinetic curves (a) and byproduct selectivities (b) for experiments with and without ultrasonic (US) pretreatment of the catalyst. Reaction conditions: 172.2 g of MBY, 50 mg of catalyst, 333 K, 0.28 MPa, 1500 rpm, baffled. US pretreatment: 1 h for the catalyst suspended in MBY.

alkynes hydrogenations.[1,36] Direct alkane formation from alkyne may proceed via multiply bound ethylidyne species that was shown by ^{14}C labeling in acetylene/ethylene hydrogenation.[37] Dimer formation stops when all MBY is consumed and does not proceed without hydrogen. Kinetic modeling was based on the reaction scheme presented in Figure 1.

Figure 7 shows the experimental points and predicted concentration versus time curves. A detailed mechanism and derivation of the kinetic equations used for modeling are presented in Supporting Information. Acetylene alcohol hydrogenations are known to be first order with respect to hydrogen,[32,38] as is its dissociative adsorption on Pt group metals.[3] To fulfill the two conditions, addition of the second hydrogen atom to the half-hydrogenated organic species should be considered as a rate-determining step, while the addition of the first atom is quasi-equilibrated as proposed in refs 3 and 39.

The transformation rate of MBY to MBE can be expressed as follows:

$$r_1 = k_1 * \frac{K_{MBY}C_{MBY}}{(1 + K_{MBY}C_{MBY} + K_H^{1/2}C_{H2}^{1/2} + K_{MBE}C_{MBE} + K_{MBA}C_{MBA} + K_D C_D)^2}$$ (9)

where $k_1* = k_1 K_{MBY-H}C_{H2}K_H$; k_1 is a reaction rate constant; and K_{MBY}, K_{MBE}, K_{MBA}, K_D, K_H, and K_{MBY-H} are the adsorption equilibrium constants of MBY, MBE, MBA, D, a hydrogen
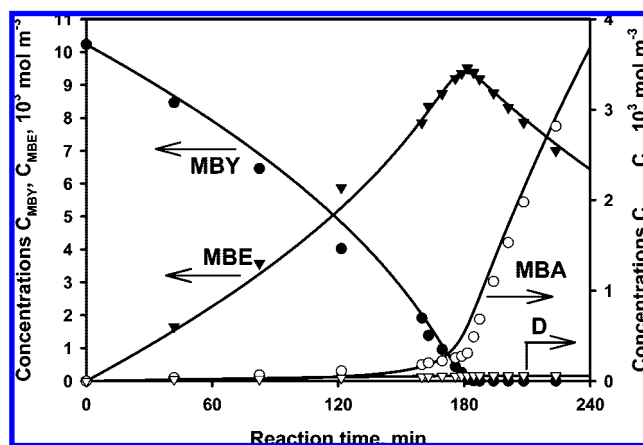

Figure 7. Kinetic curves of MBY hydrogenation with experimental points and lines from modeling. Reaction conditions: 270 g of MBY, 90 mg of catalyst, 333 K, 0.28 MPa, and 2000 rpm.

atom, and a half-hydrogenated MBY MBY-H. The dimer concentration is considerably low (maximum ∼ 0.05 M), and the adsorption constant of MBA is small; $K_{MBA}C_{MBA}$ and $K_D C_D$ can be neglected in the denominator. Taking also into consideration a weak hydrogen adsorption on Pt group metals[3] and its low bulk concentration of 0.005 M, that is, $K_H C_{H2} \ll 1$, eq 9 may be simplified as

$$r_1 = k_1 * \frac{K_{MBY}C_{MBY}}{(1 + K_{MBY}C_{MBY} + K_{MBE}C_{MBE})^2} \qquad (10)$$

For to MBE transformation to MBA and MBY to dimers, the following expressions can be developed:

$$r_2 = k_2 * \frac{K_{MBE}C_{MBE}}{(1 + K_{MBY}C_{MBY} + K_{MBE}C_{MBE})^2} \qquad (11)$$

$$r_4 = k_4 * \frac{K_{MBY}^2 C_{MBY}^2}{(1 + K_{MBY}C_{MBY} + K_{MBE}C_{MBE})^2} \qquad (12)$$

Direct hydrogenation of MBY to MBA is assumed to proceed via multiply bound intermediate species without their desorption:[1]

$$r_3 = k_3 * \frac{K_{MBY}C_{MBY}}{(1 + K_{MBY}C_{MBY} + K_{MBE}C_{MBE})^2} \qquad (13)$$

The mass balances for MBY and the reaction products are given by the following differential equations:

$$\frac{dC_{MBY}}{dt} = -\frac{m_{cat}}{V_L}(r_1 + 2r_4 + r_3) \qquad (14)$$

$$\frac{dC_{MBE}}{dt} = \frac{m_{cat}}{V_L}(r_1 - r_2) \qquad (15)$$

$$\frac{dC_{MBA}}{dt} = \frac{m_{cat}}{V_L}(r_2 + r_3) \qquad (16)$$

$$\frac{dC_D}{dt} = \frac{m_{cat}}{V_L}r_4 \qquad (17)$$

where m_{cat} is the catalyst mass and V_L is a volume of liquid phase in the reactor.

Equations 14−17 were solved numerically by the Rosenbrock method using a commercial solver (Berkeley Madonna).[40] The modeling parameters were estimated by fitting the simulated curves to the experimental data (Figure 7). The squares of the Pearson product−moment correlation coefficients (RSQ) are 0.995 for MBY kinetic curve, 0.991 for the MBE curve, 0.996 for the MBA curve, and 0.950 for the dimer kinetic curve. Calculated model parameters were $K_{MBY} = 1.03 \times 10^{-3}$ m^3·mol^{-1}, $K_{MBE} = 10^{-5}$ m^3·mol^{-1}, $k_1* = 25.3$ mol·kg$_{cat}^{-1}$·s^{-1}, $k_2* = 44.6$ mol·kg$_{cat}^{-1}$·s^{-1}, $k_3* = 5.6 \times 10^{-2}$ mol·kg$_{cat}^{-1}$·s^{-1}, and $k_4* = 2.7 \times 10^{-2}$ mol·kg$_{cat}^{-1}$·s^{-1}. The rate constant of MBE overhydrogenation to MBA, k_2, is higher than k_1 while the ratio K_{MBE}/K_{MBY} is 10^{-2}. This is in agreement with the thermodynamics for high selectivity to alkene, which is due to the stronger adsorption of the alkyne compared to the alkene and not due to the higher rate constant.[1]

4. Conclusions

(i) Mass-transfer and reaction kinetics were studied during a three-phase selective hydrogenation of 2-methyl-3-butyn-2-ol to 2-methyl-3-buten-2-ol over modified Pd/CaCO$_3$ catalyst. Determination of the intrinsic kinetic regime was performed by monitoring the dissolved hydrogen concentration via the Fugatron analyzer.

(ii) Volumetric G-L mass transfer coefficients in the absence of the catalyst were measured by gas absorption experiments for different stirrer speeds. Under the reaction conditions with a catalyst, $k_L \cdot a$ was measured at different stirrer speeds and dissolved hydrogen concentrations of 13 mol·m^{-3} and 5 mol·m^{-3}. No G-L limitations were observed at a stirrer speed

above 1500 rpm, and the dissolved H$_2$ concentration approached its value at saturation.

(iii) L-S mass transfer was analyzed by estimating Carberry numbers at various stirring intensities for two concentrations of dissolved hydrogen. Hydrogen L-S mass transfer was found to be negligible, whereas the alkyne mass transfer becomes important at its high conversions at high hydrogen concentration and low stirrer speed. Reaction conditions providing the kinetic regime could be established at low hydrogen concentration and high stirring intensity.

(iv) Modeling of the intrinsic kinetics based on the Langmuir−Hinshelwood mechanism was consistent with the experimental data obtained under the kinetic regime conditions. High selectivity to alkene could be explained by the two orders of magnitude higher adsorption constant of alkyne as compared to the one of alkene.

Supporting Information Available: Determination of the volumetric G-L mass transfer coefficient ($k_L \cdot a$) in the absence of the catalyst via gas absorption experiments; derivation of the equations used for kinetic modeling. This information is available free of charge via the Internet at http: //pubs.acs.org.

Note Added after ASAP Publication: The version of the paper that was published on the Web August 6, 2008 had errors in eq 9. The corrected version was reposted to the Web August 12, 2008.

Literature Cited

(1) Molnar, A.; Sarkany, A.; Varga, M. Hydrogenation of Carbon-Carbon Multiple Bonds: Chemo-, Regio- and Stereo-Selectivity. *J. Mol. Catal. A* **2001**, *173*, 185.

(2) Nijhuis, T. A.; van Koten, G.; Moulijn, J. A. Optimized Palladium Catalyst Systems for the Selective Liquid-Phase Hydrogenation of Functionalized Alkynes. *Appl. Catal., A* **2003**, *238*, 259.

(3) Singh, U. K.; Vannice, M. A. Liquid-Phase Hydrogenation of Citral over Pt/SiO$_2$ Catalysts. *J. Catal.* **2000**, *165−180*, 191.

(4) Roessler, F. Catalytic Hydrogenation in the Liquid Phase. *Chimia* **2003**, *57*, 791.

(5) Spee, M. P. R.; Boersma, J.; Mejer, M. D.; Slagt, M. Q.; van Koten, G.; Geus, J. W. Selective Liquid-Phase Semihydrogenation of Functionalized Acetylenes and Propargylic Alcohols with Silica-Supported Bimetallic Palladium-Copper Catalysts. *J. Org. Chem.* **2001**, *66*, 1647.

(6) Aumo, J.; Warna, J.; Salmi, T.; Murzin, D. Y. Interaction of Kinetics and Internal Diffusion in Complex Catalytic Three-Phase Reactions: Activity and Selectivity in Citral Hydrogenation. *Chem. Eng. Sci.* **2006**, *61*, 814.

(7) Cabrera, M. I.; Grau, R. J. Liquid-Phase Hydrogenation of Methyl Oleate on a Ni/α-Al$_2$O$_3$ Catalyst: A Study Based on Kinetic Models Describing Extreme and Intermediate Adsorption Regimes. *J. Mol. Catal. A* **2006**, *260*, 269.

(8) Grau, R. J.; Cassano, A. E.; Baltanas, M. A. The Cup-and-Cap Reactor: a Device to Eliminate Induction Times in Mechanically Agitated Slurry Reactors Operated with Fine Catalyst Particles. *Ind. Eng. Chem. Res.* **1987**, *26*, 18.

(9) Winterbottom, J. M.; Fishwick, R.; Stitt, H. Solid-Liquid Mass Transfer and Hydrodynamics in the Hydrogenation of 4-Nitrobenzoic Acid. *Can. J. Chem. Eng.* **2003**, *81*, 588.

(10) Mukherjee, S.; Vannice, M. A. Solvent Effects in Liquid-Phase Reactions. I. Activity and Selectivity During Citral Hydrogenation on Pt/SiO$_2$ and Evaluation of Mass Transfer Effects. *J. Catal.* **2006**, *243*, 108.

(11) Singh, U. K.; Vannice, M. A. Kinetics of Liquid-Phase Hydrogenation Reactions over Supported Metal Catalysts - a Review. *Appl. Catal., A* **2001**, *213*, 1.

(12) Nijhuis, T. A.; van Koten, G.; Kapteijn, F.; Moulijn, J. A. Separation of Kinetics and Mass-Transport Effects for a Fast Reaction: the Selective Hydrogenation of Functionalized Alkynes. *Catal. Today* **2003**, *79−80*, 315.

(13) Gavroy, D.; Jolyvuillemin, C.; Cordier, G.; Fouilloux, P.; Delmas, H. Continuous Hydrogenation of Adiponitrile on Raney-Nickel in a Slurry Bubble-Column. *Catal. Today* **1995**, *24*, 103.

(14) Meyberg, M.; Roessler, F. In Situ Measurement of Steady-State Hydrogen Concentrations During a Hydrogenation Reaction in a Gas-Inducing Stirred Slurry Reactor. *Ind. Eng. Chem. Res.* **2005**, *44*, 9705.

(15) Beenackers, A. A. C. M.; Van Swaaij, W. P. M. Mass Transfer in Gas - Liquid Slurry Reactors. *Chem. Eng. Sci.* **1993**, *48*, 3109.

(16) Scharringer, P.; Muller, T. E.; Kaltner, W.; Lercher, J. A. In Situ Measurement of Dissolved Hydrogen During the Liquid-Phase Hydrogenation of Dinitriles - Method and Case Study. *Ind. Eng. Chem. Res.* **2005**, *44*, 9770.

(17) 3-buten-2-ol, 2-methyl, CAS No. 115-18-4, UNEP Publications.

(18) Semagina, N.; Grasemann, M.; Xanthopoulos, N.; Renken, A.; Kiwi-Minsker, L. Structured Catalyst of Pd/ZnO on Sintered Metal Fibers for 2-Methyl-3-Butyn-2-ol Selective Hydrogenation. *J. Catal.* **2007**, *251*, 213.

(19) Bronstein, L. M.; Chernyshov, D. M.; Volkov, I. O.; Ezernitskaya, M. G.; Valetsky, P. M.; Matveeva, V. G.; Sulman, E. M. Structure and Properties of Bimetallic Colloids Formed in Polystyrene- Block-Poly-4-Vinylpyridine Micelles: Catalytic Behavior in Selective Hydrogenation of Dehydrolinalool. *J. Catal.* **2000**, *196*, 302.

(20) Lide, D. R. *CRC Handbook of Chemistry and Physics*; CRC Press LLC: Boca Raton, 2001.

(21) Sporka, K.; Hanika, J.; Ruzicka, V. Diffusion of Gases in Liquids. Measurement of the Diffusion Coefficient of Hydrogen in Alcohols. *Collect. Czech. Chem. Commun.* **1969**, *34*, 3145.

(22) Liley, P. E.; Thompson, G. H.; Friend D. G.; Daubert, T. E.; Buck, E. Physical and Chemical Data. In *Perry's Chemical Engineers' Handbook*; Perry, R. H., Green, D. W., Maloney, J. O., Eds.; McGraw-Hill: Singapore, 1997.

(23) Dollimore, D.; Heal, G. R. Improved Method for Calculation of Pore Size Distribution from Adsorption Data. *J. Appl. Chem. USSR* **1964**, *14*, 109.

(24) Deimling, A.; Karandikar, B. M.; Shah, Y. T. Solubility and Mass transfer of CO and H$_2$ in Fischer−Tropsch Liquids and Slurries. *Chem. Eng. J.* **1984**, *29*, 127.

(25) Reichert, C.; Hoell, W. H.; Franzreb, M. Mass Transfer Enhancement in Stirred Suspensions of Magnetic Particles by the Use of Alternating Magnetic Fields. *Powder Technol.* **2004**, *145*, 131.

(26) Junmei, Z.; Chunjian, X.; Ming, Z. The Mechanism Model of Gas-Liquid Mass Transfer Enhancement by Fine Catalyst Particles. *Chem. Eng. J.* **2006**, *120*, 149.

(27) Emig, G.; Dittmeyer, R. Simultaneous Heat and Mass Transfer and Chemical Reaction. In *Handbook of Heterogeneous Catalysis*; Ertl, G., Knözinger, H., Weitkamp, J., Eds.; VCH Verlagsgesellschaft mbH: Weinheim, Germany, 1997; Vol. III.

(28) Vannice, M. A. *Kinetics of catalytic reactions*; Springer: New York, 2005.

(29) Sano, Y.; Yamaguchi, N.; Adachi, T. Mass Transfer Coefficients for Suspended Particles in Agitated Vessels and Bubble Columns. *J. Chem. Eng. Jpn.* **1974**, *7*, 255.

(30) Bates, R. C.; Fondy, P. L.; Corpstein, R. R. An Examination of Some Geometric Parameters of Impeller Power. *Ind. Eng. Chem. Proc. Des. Dev.* **1963**, *3*, 310.

(31) Schlogl, R.; Noack, K.; Zbinden, H.; Reller, A. The Microstructure of Selective Palladium Hydrogenation Catalysts Supported on Calcium Carbonate and Modified by Lead (Lindlar Catalysts), Studied by Photoelectron Spectroscopy, Thermogravimetry, X-ray Diffraction, and Electron Microscopy. *Helv. Chim. Acta* **1987**, *70*, 627.

(32) Sulman, E. M. Selective Hydrogenation of Unsaturated Ketones and Acetylene Alcohols. *Russ. Chem. Rev.* **1994**, *63*, 923.

(33) Joannet, E.; Horny, C.; Kiwi-Minsker, L.; Renken, A. Palladium Supported on Filamentous Active Carbon as Effective Catalyst for Liquid-Phase Hydrogenation of 2-Butyne-1,4-Diol to 2-Butene-1,4-Diol. *Chem. Eng. Sci.* **2002**, *57*, 3453.

(34) Chaudhari, R. V.; Parande, M. G.; Ramachandran, P. A.; Brahme, P. H.; Vagaonkar, H. G.; Jaganathan, R. Hydrogenation of Butynediol to Cis-Butenediol Catalyzed by Pd-Zn-CaCO$_3$: Reaction Kinetics and Modeling of a Batch Slurry Reactor. *AIChE J.* **1985**, *31*, 1891.

(35) Mukherjee, S.; Vannice, M. A. Solvent Effects in Liquid-Phase Reactions. II. Kinetic Modeling for Citral Hydrogenation. *J. Catal.* **2006**, *243*, 131.

(36) Semagina, N.; Renken, A.; Laub, D.; Kiwi-Minsker, L. Synthesis of Monodispersed Palladium Nanoparticles to Study Structure Sensitivity of Solvent-Free Selective Hydrogenation of 2-Methyl-3-Butyn-2-ol. *J. Catal.* **2007**, *246*, 308.

(37) Leviness, S.; Nair, V.; Weiss, A. H.; Schay, Z.; Guczi, L. Acetylene Hydrogenation Selectivity Control on PdCu/Al$_2$O$_3$ Catalysts. *J. Mol. Catal.* **1984**, *25*, 131.

(38) Semagina, N.; Joannet, E.; Parra, S.; Sulman, E.; Renken, A.; Kiwi-Minsker, L. Palladium Nanoparticles Stabilized in Block-Copolymer Micelles for Highly Selective 2-Butyne-1,4-Diol Partial Hydrogenation. *Appl. Catal., A* **2005**, *280*, 141.

(39) Gonsalves, K. E.; Li, H.; Perez, R.; Santiago, P.; Jose-Yacaman, M. Synthesis of Nanostructured Metals and Metal Alloys from Organometallics. *Coord. Chem. Rev.* **2000**, *206−207*, 607.

(40) Macey, R. I.; Oster, G. F. *Berkeley Madonna*; University of California: Berkeley, CA, 1997−2001.